Effect of Alpine glaciation on thermochronometer age-elevation profiles

Mathew S. Densmore,[1] Todd A. Ehlers,[1] and Glenn J. Woodsworth[2]

[1] Low-temperature thermochronometers are widely used to quantify exhumation histories, typically by interpreting sample cooling age-elevation relationships. However, the effects of specific geomorphic processes on age-elevation profiles are seldom considered. We integrate apatite (U-Th)/He [AHe], apatite fission track, and zircon (U-Th)/He thermochronometry with numerical modeling to determine the effect of glacial erosion on an age-elevation profile from the heavily glaciated southern Coast Mountains, British Columbia. AHe data show a distinct break in slope in age-elevation between 1900–2100 m. We interpret this break in slope as an acceleration of erosion associated with the onset of alpine glaciation. We use a 3-D thermo-kinematic model to constrain pre- and synglacial erosion rates. Results indicate a preglacial erosion rate of ∼0.4 mm/yr that accelerated by a factor of ∼2 since ∼6 Ma. We propose that glacial valley widening and deepening are responsible for the observed nonlinear AHe age-elevation profile. **Citation:** Densmore, M. S., T. A. Ehlers, and G. J. Woodsworth (2007), Effect of Alpine glaciation on thermochronometer age-elevation profiles, *Geophys. Res. Lett.*, *34*, L02502, doi:10.1029/2006GL028371.

1. Introduction

[2] Low-temperature thermochronometers are proven tools for quantifying long-term ($\sim 10^4 - 10^7$ years) exhumation processes [e.g., *Hodges*, 2003]. The most common method for thermochronometer interpretation is analysis of sample cooling age versus elevation [e.g., *Wagner et al.*, 1977]. Exhumation rates are calculated from the slope of the best-fit line through an age-elevation profile. Linear age-elevation relationships are interpreted as indicating uniform exhumation. A break in slope suggests a change in exhumation rate, presumably associated with a tectonic or erosional mechanism [e.g., *Fitzgerald et al.*, 1995]. Despite the widespread application of these techniques to tectonic studies, few studies have quantified long-term glacial erosion [e.g., *Meigs and Sauber*, 2000; *Spotila et al.*, 2004; *Thomson*, 2002] and no study has examined the effect of a specific geomorphic process on age-elevation profiles.

[3] Glaciers are efficient agents of erosion and should influence erosion rates and thermochronometer age-elevation relationships. Long-term glacial erosion-rate estimates are based primarily on sediment flux data collected over decadal to millennial timescales (max. 2100 yrs), span three orders of magnitude from 0.01 to >60 mm/yr, and hence are highly variable [*Hallet et al.*, 1996]. Erosion rates between 10 – 60 mm/yr are difficult to sustain over the Quaternary because they predict unobserved large magnitudes of erosion (20 – 120 km) and suggest exposure of mantle material.

[4] We use a comparison between numerical model predicted and observed cooling ages from a heavily glaciated valley flank in the Coast Mountains, British Columbia, to quantify the effect of glacial valley widening and deepening on age-elevation profiles.

2. Geologic Setting

[5] The Coast Mountains are located on the west coast of Canada, extending over 1,000 km from Vancouver to southern Alaska, USA (Figure 1a). Major glaciated valleys traverse the range, with onset of alpine glaciation in the southern Alaskan region inferred to be ∼9 Ma from lava flows within tillites [*Denton and Armstrong*, 1969]. Although less clear, glaciation in the southern Coast Mountains is thought to have occurred since the latest Miocene [*Clague*, 1991].

[6] The Mount Waddington region (Figure 1b) is well suited for applying low-temperature thermochronometry to quantify glacial erosion [*Ehlers et al.*, 2006]. This region has been heavily glaciated without significant faulting [*Farley et al.*, 2001; *Sweeney et al.*, 1992], resulting in a purely erosional exhumation mechanism for thermochronometer cooling. The predominantly mid Jurassic to Eocene tonalites and granodiorites [*Woodsworth et al.*, 1991] yield pristine grains for apatite (U-Th)/He [AHe], apatite fission track [AFT] and zircon (U-Th)/He [ZHe] analysis, resulting in reproducible cooling ages (average 1σ error is ∼9 % for AHe; Table S1 in the auxiliary material[1]).

[7] Previous studies have documented the Neogene exhumation history within the Coast Mountains (Figure 1a). AFT and zircon fission-track studies by *Parrish* [1983] and *O'Sullivan and Parrish* [1995] characterized the cooling history in the Mt. Waddington region from ∼30 – 8 Ma. *Shuster et al.* [2005] determined ∼2 km of erosion since 1.8 Ma by applying ^{4}He/^{3}He thermochronometry to some of the samples presented here. *Ehlers et al.* [2006] demonstrate that large magnitude and accelerated glacial erosion was pervasive across the southern Coast Mountains. This study complements previous work by addressing how glacial erosion influences thermochronometer age-elevation profiles.

3. Method and Observations
3.1. Low-Temperature Thermochronology

[8] Low-temperature thermochronometers record cooling through the upper crust and are sensitive to, among other

---

[1]Department of Geological Sciences, University of Michigan, Ann Arbor, Michigan, USA.
[2]Geological Survey of Canada, Vancouver, British Columbia, Canada.

---

things, perturbations of the thermal field from topography [*Braun*, 2005; *Ehlers and Farley*, 2003]. Topography can alter the background thermal field of the upper crust by increasing thermal gradients beneath valleys relative to interfluves [*Lees*, 1910; *Stuwe et al.*, 1994]. Each thermo-
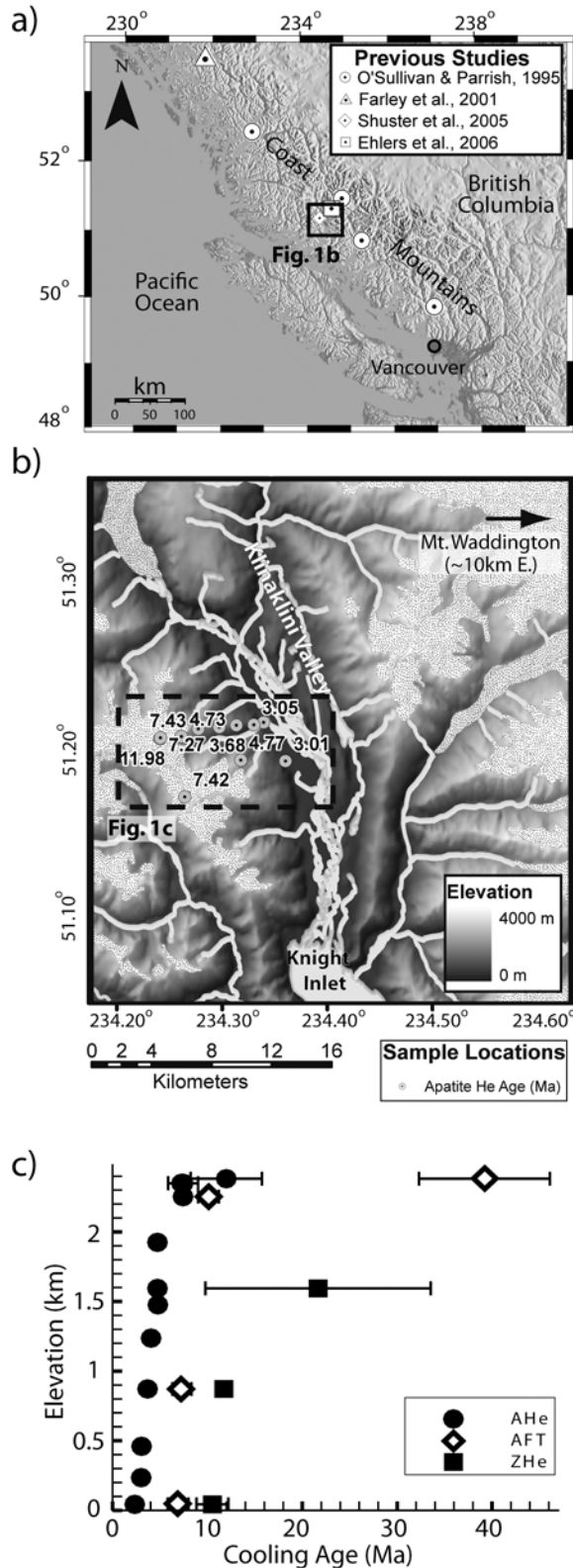

Figure 1. Topography and thermochronometer data in the Coast Mountains, British Columbia. (a) Shaded relief DEM with locations of previous studies. (b) Study area in the previously glaciated Klinaklini Valley with a vertical transect of new sample locations and cooling ages. Shaded relief DEM includes snow and ice coverage (stipple pattern). (c) Apatite (U-Th)/He [AHe], apatite fission track [AFT] and zircon (U-Th)/He [ZHe] cooling ages versus sample elevation. 1σ error bars contained within symbol if not visible.
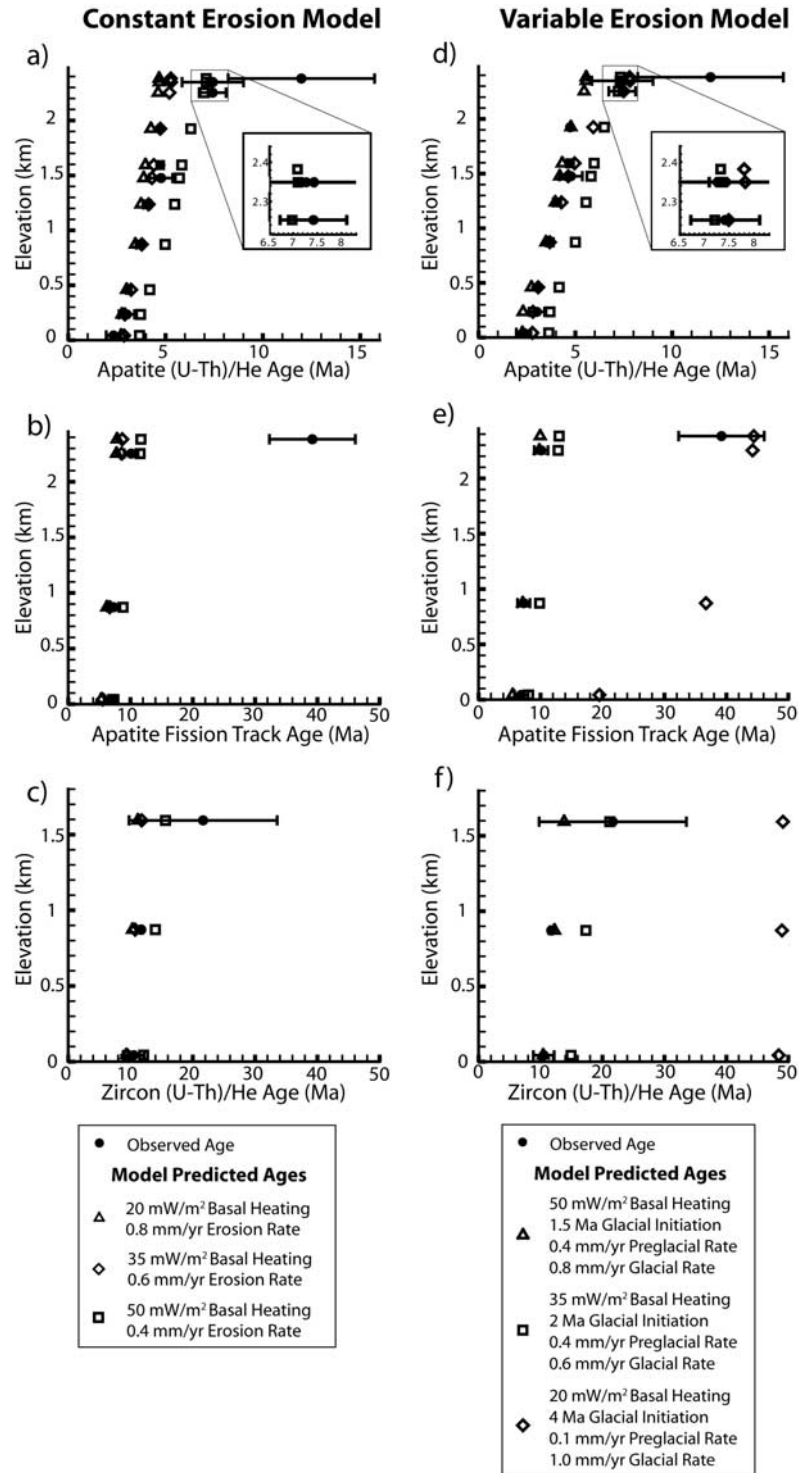
chronometer system is sensitive to a cooling rate dependent closure temperature, so as a sample is exhumed, it will record the time elapsed since passing through this closure temperature [*Dodson*, 1973]. Combining multiple low-temperature thermochronometer systems can provide a robust and detailed exhumation history through the upper crust [*Reiners et al.*, 2003]. Because higher temperature systems require more time to be exhumed from their closure temperature to the surface, this multiple systems approach can characterize the exhumation history in this part of the Coast Mountains over ~15 Myr, and therefore capture both the pre- and synglacial erosion regimes.

3.2. Data

[9] We present new analyses for twelve samples from a single vertical transect on the western flank of the Klinaklini River Valley (Figure 1b). We sampled the 2300 m vertical extent across a lateral distance of 2500 m. All twelve samples were analyzed for AHe, four were analyzed for AFT, and three for ZHe (Figure 1c and Tables S1, S2, and S3; see auxiliary material for data tables and analytical methods). AHe cooling ages range from 2.3 – 12.0 Ma, with average 1σ error of ~9%. Additionally, the AFT and ZHe cooling ages range from 6.9 – 39.2 Ma, and 10.5 – 21.7 Ma, respectively. Average 1σ errors are 15% for AFT ages and 23% for ZHe.

[10] A distinct break in slope in the age-elevation profile is evident in both the measured AHe and AFT ages. For the AHe data, this break occurs at ~2000 m elevation (Figures 2a and 2d), corresponding to a sample age of ~6 Ma, and consistent with estimates for the onset of alpine glaciation in this region. A linear regression through this data yields an apparent exhumation rate of ~0.03 mm/yr prior to ~5.5 Ma, accelerating to ~0.7 mm/yr for the period between 1.98 and ~5.5 Ma. Similarly, the AFT data show a break in slope occurring at 2400 m, corresponding to an age of 12 – 20 Ma (Figures 2b and 2e). However, comparison of fission track lengths show long mean lengths (~14.20 ± 0.15 μm) for the three lower samples and shorter lengths (13.26 ± 0.19 μm) for the top sample (Table S2 of the auxiliary material) suggesting this sample represents the base of an exhumed partial annealing zone [*Gallagher et al.*, 1998] and not a rate increase (see auxiliary material for detailed discussion of this sample).

3.3. Thermo-Kinematic Model

[11] Quantifying exhumation histories from thermochronometer data can be complicated by temporal and spatial variations in the thermal field samples cool through [*Mancktelow and Grasemann*, 1997], which can result from

Figure 2. Comparison of observed and predicted thermochronometer age-elevation profiles. (a and d) AHe, (b and e) AFT, and (c and f) ZHe. Observed (filled circles) and predicted (open symbols) cooling ages for (Figures 2a, 2b, and 2c) uniform and (Figures 2d, 2e, and 2f) temporally variable erosion rates. 1σ error bars contained within symbol if not visible. Constant erosion-rate models do not predict a break in slope in the AHe data. We highlight three variable erosion models. Two models (open triangles and squares in Figures 2d–f) bound a region where many parameter combinations yield similar fits (Table S4 in the auxiliary material). One model (diamonds) fits the AHe data in Figure 2d, however, the higher temperature systems show significant offset in Figures 2e and 2f. Temporally variable erosion models can predict a break in slope but underpredict its magnitude.

variations in the exhumation rate, and/or topography. We use a 3D thermo-kinematic finite element model to quantify the effect of these perturbations on the thermal field, rock cooling histories, and thermochronometer cooling ages [*Braun*, 2005; *Ehlers and Farley*, 2003; *Ehlers et al.*, 2006; *Kohl and Hopkirk*, 1995]. The model solves the 3D advection-diffusion equation with heat production to determine the heat transfer between elements. Details of the modeling approach are given in the auxiliary material and salient points are summarized here.

[12] The approach followed here is to explore the simplest case of static topography and use differences between predicted and observed thermochronometer ages to infer landscape evolution processes. Future work will use these results to guide simulations that account for the more difficult case of evolving topography. Free parameters in the thermal model include internal heat production (0.8 μW/m^3) and thermal conductivity (2.7 W/mK) [*Lewis et al.*, 1985]. The initial condition of the thermal model is a purely conductive steady-state thermal field [*Ehlers et al.*, 2006] using basal heat flow (20 – 50 mW/m^2) [*Lewis et al.*, 1985] and a constant elevation-dependent surface temperature (T = 4°C at sea level). A transient thermal solution is calculated while samples undergo vertical exhumation at a specified rate for 20 Myr, using a nominal initial age of 50 Ma. Lack of evidence for major active faulting justifies the assumption of purely vertical exhumation.

[13] Simulations were conducted with varying erosion rates from 20 Ma to present. Range of free parameters explored in the kinematic model include pre- and synglacial erosion rates (0.2 – 0.8 and 0.2 – 1.0 mm/yr, respectively), and a variable onset time of glaciation (1.5 – 8 Ma). Particles corresponding to sample locations are tracked backwards through time from the surface into the model interior and the thermal histories are recorded. Using TERRA [*Ehlers et al.*, 2005], each particle time-temperature history is used to predict AHe, AFT and ZHe cooling ages with He diffusion and fission track annealing algorithms.

4. Results

[14] We tested 210 combinations of model parameters described above in order to explore two erosional scenarios including: (1) spatially and temporally constant erosion, representing a stable long-term erosional regime, and (2) spatially constant but temporally variable erosion, representing an increase in rate due to glaciation. Rock advection velocities are held constant until a defined threshold time at which point the velocities either remain constant or are increased to represent glaciation. Model output from a given set of free parameters is not unique and represents the tradeoff between variables. Due to this non-uniqueness, we tested across the entire parameter space to identify combinations of parameters that minimize the difference between predicted and observed AHe, AFT, and ZHe ages. We quantified the goodness of fit of each model run with a statistical reduced χ^2 analysis [*Ehlers et al.*, 2003]. The χ^2 value is a one-sided distribution, where a value of zero indicates a perfect fit, and higher values represent a progressively worse fit. We calculated χ^2 values for AHe ages only, as there are too few AFT and ZHe ages to compare to

model parameters (equation (2) in the auxiliary material). Our criteria for an adequate model are: (1) a χ^2 value below 5.0 (25th percentile), and (2) under-predicting no more than one AHe age.

4.1. Scenario 1: Spatially and Temporally Constant Erosion

[15] This scenario considers the simplest case of steady-state erosion. Each simulation explored a different constant erosion rate ranging between 0.2–1.0 mm/yr, for 20 Myr. In the case of exhumation at a constant rate, only rates of 0.6 and 0.8 mm/yr predict cooling ages that adequately fit most of the low-elevation AHe data (Figure 2a). For the higher temperature systems, these rates under-predict all observed cooling ages and generate strictly linear profiles. Although a slower rate of 0.4 mm/yr generates predicted ages that roughly match the AHe data above 2 km, low-elevation ages for all three systems are over-predicted (Figures 2a, 2b, and 2c, squares). Results from this set of models generally yield poor fits to the data with no combinations predicting a break in slope as observed in the AHe data at >2 km elevation. Although some misfit occurs, these model results suggest a long-term (>5 Ma) average erosion rate of roughly 0.4 mm/yr and a short-term (<5 Ma) rate of ~0.6 – 0.8 mm/yr.

4.2. Scenario 2: Spatially Constant but Temporally Variable Erosion

[16] This scenario evaluates how variations in pre- and synglacial erosion rates influence age-elevation profiles. Several combinations of pre- and synglacial erosion rates, and onset times for glaciation generated an adequate fit to the observed AHe data at elevations below 2 km (see Table S4 of the auxiliary material for detailed results). Models with an average initial velocity of ~0.4 accelerating to ~0.8 mm/yr at ~4 Ma generated age-elevation profiles close to the data and fall between the triangle and square symbols plotted on Figure 2d. The large number of adequately fitting model combinations is reduced when ZHe data is considered by eliminating models with low initial exhumation rates (< 0.4 mm/yr). Predicted ZHe cooling ages require an initial rate of ~0.4 mm/yr to produce enough exhumation to replicate these higher temperature data.

[17] However, no model explored in scenario (2) predicted cooling ages with a break in slope of AHe data similar in magnitude to that observed, although several did produce very subtle breaks in the predicted age-elevation profiles. For example, Figure 2d shows two such model runs (triangles and squares) where the top two samples fall slightly off trend from the lower samples. In order to determine the initial rate required to produce a comparable break in slope, an additional model was conducted with an initial exhumation rate of 0.1 accelerating to 1.0 mm/yr at 4 Ma (Figures 2d, 2e, and 2f, diamonds). This model predicts AHe cooling ages very similar to those observed at both high and low elevations. However, AFT ages are significantly over-predicted by at least 14 Myr. Furthermore, the predicted ZHe ages poorly fit the data as well, with a 30 Myr misfit. Thus, although an order of magnitude variation between pre- and synglacial erosion rates improves the fit to the AHe data it fails to erode enough material to produce the observed AFT and ZHe ages.
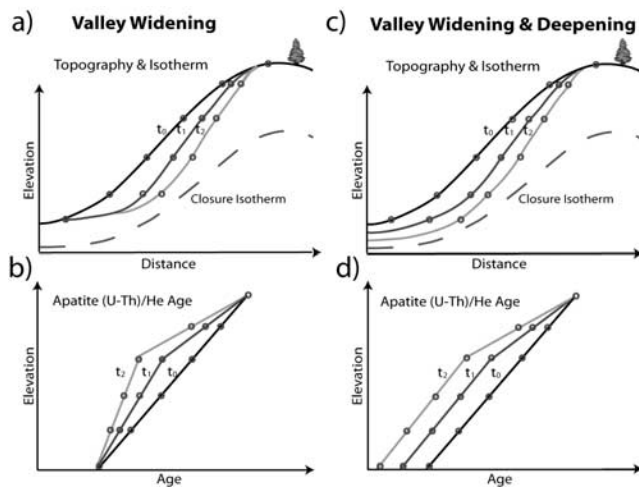
Figure 3. Schematic diagram of glacial valley widening and deepening and the effect on thermochronometer age-elevation profiles. Temporal evolution is from initial time t_0 to final time t_2. (a) At all intermediate elevations valley widening reduces the distance traveled from a closure isotherm and (b) decreases the cooling ages. (c) Coupled widening and deepening lowers the valley floor and (d) decreases the corresponding cooling ages. The relative age of the lowest elevation sample may indicate whether Figure 3a widening or Figure 3c coupled widening and deepening is the dominant process.

[18] Although implementing temporally variable exhumation in the model does result in similar cooling ages to those observed, the systematic misfit of high-elevation samples suggest that the erosional history is more complex than assumed in these scenarios. To create enough erosion to exhume relatively young AFT and ZHe samples, the long-term erosion rate must be sufficiently high (~0.4 mm/yr). However, in order to produce a significant offset in AHe ages at high elevations, the erosion rate must increase at low elevations while remaining constant or perhaps decreasing at high elevations. This rate change must occur at ~6 Ma to avoid exhumation of AFT and ZHe samples that are younger than we observe. These observations indicate a spatially and temporally variable erosion rate is required in order to reproduce the observed trends in cooling ages.

5. Discussion

[19] In this section, we present a scenario whereby glacial erosion can produce a break in slope of an age-elevation profile and compare our results with previous studies in the Coast Mountains.

5.1. Spatial Variations in Glacial Erosion

[20] Our results suggest a low pre-glacial erosion rate until ~6 Ma, followed by a factor of ~2 increase in erosion at low elevations (<2000 m). The most likely mechanism for this pattern of erosion is by glacial valley widening and deepening. *Hallet* [1979] suggested glacial erosion is a function of basal ice velocity. Within the Coast Mountains, ice was thick enough to induce pressure melting at the base of large glaciers [*Booth*, 1986; *Ehlers et al.*, 2006], therefore increasing basal-sliding velocity and valley bottom erosion relative to valley

walls. Application of this velocity dependent glacial erosion law in numerical models [*Harbor*, 1992] suggests that large, km, scale glacial valley widening and deepening can occur rapidly, and on timescales less than 10^6 yr.

[21] Coupling a glacial landscape evolution and thermal model is an alternative approach to quantifying the effect of glaciation on age-elevation profiles. However, this approach is well beyond the scope of this study and the focus of work in progress. Rather, here we present a conceptual model for the effect of glaciation on low-temperature thermochronometer age-elevation profiles. Figure 3 illustrates how glacial valley widening and deepening can influence these profiles. Considering only the effect of valley widening, the topography is modified as glaciers erode the valley wall while not changing the elevation of the valley floor and ridge top (Figure 3a). If erosion outpaces thermal equilibration in the subsurface, excluding the endpoints the distance all samples travel from the closure isotherm to the surface is reduced, decreasing their cooling ages (Figure 3b). In contrast, combined valley widening and deepening causes the valley floor to also be eroded (Figure 3c) so all but the highest elevation sample age is reduced (Figure 3d).

[22] The effects of valley widening and deepening on age-elevation profiles are similar even though they differ in how they spatially distribute erosion within a valley. Both processes produce a break in slope similar to the observed AHe data. However, the primary difference between the resultant profiles is the reduced age of the bottom sample. In our data, this sample yields a relatively young AHe age, implying some component of deepening. However, without knowledge of the preglacial elevations for each sample we cannot quantify the effect of deepening on this lowest sample. Therefore, we suggest that some combination of these effects results in the observed age-elevation profile.

5.2. Comparison to Previous Work

[23] Our finding of an increase in exhumation rates from ~0.4 – 0.8 mm/yr at ~6 Ma is similar to previous exhumation studies in the Coast Mountains (Figure 1a). For example, in the northern Coast Mountains, *Farley et al.* [2001] document from AHe data an increase in exhumation after ~4 Ma. In the southern Coast Mountains, Mt. Waddington region, *O'Sullivan and Parrish* [1995] document rapid exhumation at ~5–8 Ma from AFT data, and *Ehlers et al.* [2006] found from bulk AHe ages a minimum 300% increase in erosion rates starting between 1.5 – 7 Ma. At the same location as this study, *Shuster et al.* [2005] applied $^4He/^3He$ thermochronometry and found a rapid increase in erosion from ~0.5 – 2.5 mm/yr at 1.8 ± 0.2 Ma. In general, our results are consistent with the previous studies in suggesting an acceleration in Neogene erosion rates. The difference in the magnitude of the acceleration between *Shuster et al.* [2005] and this study results from the bulk AHe ages used here producing erosion rates averaged over the cooling age of the sample, whereas $^4He/^3He$ thermochronometry is sensitive to discrete thermal histories.

6. Conclusions

[24] In this study we suggest that glaciation can significantly alter low-temperature thermochronometer age-elevation relationships. We present AHe, AFT and ZHe

cooling ages with distinct breaks in slope of age-elevation profiles corresponding to ~6 Ma for AHe and 12–20 Ma for AFT. We interpret the break in slope of our AHe data to reflect an acceleration of erosion below 2000 m associated with the inception of alpine glaciation in the past ~6 My. By combining 3-D thermal kinematic modeling with low-temperature thermochronometer cooling age data, we explored erosional scenarios of: (1) spatially and temporally constant rates, and (2) spatially constant, but temporally variable rates. We constrain erosion rates from ~0.4 mm/yr, increasing to ~0.8 mm/yr during the early Pliocene. This contrasts with the long-term (>6 Ma) rate of 0.03 mm/yr determined by best-fit regression line. However, neither modeling scenario investigated completely fit the data, suggesting the need for spatially and temporally variable erosion with higher rates at lower (<2000 m) elevations. If erosion rates are higher within valleys compared to adjacent ridges, a break in slope will likely form in the thermochronometer age-elevation relationships. Finally, we suggest that glacial valley widening and deepening are responsible for the nonlinear age-elevation profile in our AHe data and suggest glaciation may have a similar influence on AHe age-elevation profiles collected in other heavily glaciated regions.

References

Booth, D. B. (1986), Mass balance and sliding velocity of the Puget Lobe of the Cordilleran ice sheet during the last Glaciation, *Quat. Res.*, *25*, 269–280.

Braun, J. (2005), Quantitative constraints on the rate of landform evolution derived from low-temperature thermochronology, in *Low-Temperature Thermochronology: Techniques, Interpretations, and Applications*, *Rev. Mineral. Geochem.*, vol. 58, edited by P. W. Reiners and T. A. Ehlers, pp. 351–374, Mineral. Soc. of Am., Washington, D. C.

Clague, J. J. (1991), Quaternary glaciation and sedimentation, in *Geology of Canada*, vol. 4, *Geology of the Cordilleran Orogen in Canada*, edited by H. Gabrielse and C. J. Yorath, pp. 421–434, Geol. Surv. of Can., Ottawa.

Denton, G. H., and R. L. Armstrong (1969), Miocene-Pliocene glaciations in southern Alaska, *Am. J. Sci.*, *267*(10), 1121–1142.

Dodson, M. (1973), Closure temperature in cooling geochronological and petrological systems, *Contrib. Mineral. Petrol.*, *40*(3), 259–274.

Ehlers, T., and K. A. Farley (2003), Apatite (U-Th)/He thermochronometry: Methods and applications to problems in tectonic and surface processes, *Earth Planet. Sci. Lett.*, *206*(1–2), 1–14.

Ehlers, T. A., S. D. Willett, P. A. Armstrong, and D. S. Chapman (2003), Exhumation of the central Wasatch Mountains, Utah: 2. Thermokinematic model of exhumation, erosion, and thermochronometer interpretation, *J. Geophys. Res.*, *108*(B3), 2173, doi:10.1029/2001JB001723.

Ehlers, T., et al. (2005), Computational tools for low-temperature thermochronometer interpretation, in *Low-Temperature Thermochronology: Techniques, Interpretations, and Applications*, *Rev. Mineral. Geochem.*, vol. 58, edited by P. W. Reiners and T. A. Ehlers, pp. 589–622, Mineral. Soc. of Am., Washington, D. C.

Ehlers, T. A., et al. (2006), Apatite (U-Th)/He signal of large-magnitude accelerated glacial erosion, southwest British Columbia, *Geology*, *34*(9), 765–768.

Farley, K. A., et al. (2001), Post-10 Ma uplift and exhumation of the northern Coast Mountains, British Columbia, *Geology*, *29*(2), 99–102.

Fitzgerald, P. G., R. B. Sorkhabi, T. F. Redfield, and E. Stump (1995), Uplift and denudation of the central Alaska Range: A case study in the use of apatite fission track thermochronology to determine absolute uplift parameters, *J. Geophys. Res.*, *100*(B10), 20,175–20,192.

Gallagher, K., et al. (1998), Fission track analysis and its applications to geological problems, *Annu. Rev. Earth Planet. Sci.*, *26*, 519–572.

Hallet, B. (1979), A theoretical model of glacial abrasion, *J. Glaciol.*, *23*(89), 39–50.

Hallet, B., et al. (1996), Rates of erosion and sediment evacuation by glaciers: A review of field data and their implications, in *Global and Planetary Change*, edited by A. Solheim, et al., pp. 213–235, Elsevier, New York.

Harbor, J. M. (1992), Numerical modeling of the development of U-shaped valleys by glacial erosion, *Geol. Soc. Am. Bull.*, *104*, 1364–1375.

Hodges, K. V. (2003), Geochronology and thermochronology in orogenic systems, in *Treatise on Geochemistry*, edited by R. Rudnick, pp. 263–292, Elsevier, New York.

Kohl, T., and J. Hopkirk (1995), "FRACTure"—A simulation code for forced fluid flow and transport in fractured, porous rock, *Geothermics*, *24*(3), 333–343.

Lees, C. H. (1910), On the isogeotherms under mountain ranges in radio-active districts, *Proc. R. Soc.*, *83*, 339–346.

Lewis, T., et al. (1985), Heat flux measurements in southwestern British Columbia: The thermal consequences of plate tectonics, *Can. J. Earth Sci.*, *22*(9), 1262–1273.

Mancktelow, N., and B. Grasemann (1997), Time-dependent effects of heat advection and topography on cooling histories during erosion, *Tectonophysics*, *270*(3–4), 167–195.

Meigs, A., and J. Sauber (2000), Southern Alaska as an example of the long-term consequences of mountain building under the influence of glaciers, *Quat. Sci. Rev.*, *19*(14–15), 1543–1563.

O'Sullivan, P., and R. Parrish (1995), The importance of apatite composition and single-grain ages when interpreting fission track data from plutonic rocks: A case study from the Coast Ranges, British Columbia, *Earth Planet. Sci. Lett.*, *132*(1–4), 213–224.

Parrish, R. R. (1983), Cenozoic thermal evolution and tectonics of the Coast Mountains of British Columbia: 1. Fission track dating, apparent uplift rates, and patterns of uplift, *Tectonics*, *2*(6), 601–631.

Reiners, P. W., et al. (2003), Post-orogenic evolution of the Dabie Shan, eastern China, from (U-Th)/He and fission track thermochronology, *Am. J. Sci.*, *303*, 489–518.

Shuster, D. L., et al. (2005), Rapid glacial erosion at 1.8 Ma revealed by $^4He/^3He$ thermochronometry, *Science*, *310*(5754), 1668–1670.

Spotila, J. A., et al. (2004), Long-term glacial erosion of active mountain belts: Example of the Chugach-St. Elias Range, Alaska, *Geology*, *32*(6), 501–504.

Stuwe, K., et al. (1994), The influence of eroding topography on steady-state isotherms: Application to fission track analysis, *Earth Planet. Sci. Lett.*, *124*(1–4), 63–74.

Sweeney, J. F., et al. (1992), Tectonic framework. part C: Crustal geophysics, in *Geology of Canada*, vol. 4, *Geology of the Cordilleran Orogen in Canada*, edited by H. Gabrielse and C. J. Yorath, pp. 39–53, Geol. Surv. of Can., Ottawa.

Thomson, S. N. (2002), Late Cenozoic geomorphic and tectonic evolution of the Patagonian Andes between latitudes 42°S and 46°S: An appraisal based on fission-track results from the transpressional intra-arc Liquine-Ofqui fault zone, *Geol. Soc. Am. Bull.*, *114*(9), 1159–1173.

Wagner, G. W., et al. (1977), Cooling ages derived by apatite fission-track, mica Rb-Sr and K-Ar dating: The uplift and cooling history of the Central Alps, *Mem. Ist. Geol. Mineral. Univ. Padova*, *30*, 1–27.

Woodsworth, G. J., et al. (1991), Plutonic regimes, in *Geology of Canada*, vol. 4, *Geology of the Cordilleran Orogen in Canada*, edited by H. Gabrielse and C. J. Yorath, pp. 493–530, Geol. Surv. of Can., Ottawa.

_____

M. S. Densmore and T. A. Ehlers, Department of Geological Sciences, University of Michigan, 2534 C. C. Little Building, 100 N. University Avenue, Ann Arbor, MI 48109, USA. (mdens@umich.edu)

G. J. Woodsworth, Geological Survey of Canada, 101-605 Robson Street, Vancouver, BC, Canada V6B 5J3.